Dyes and Pigments 137 (2017) 293–298

Contents lists available at ScienceDirect

Dyes and Pigments

journal homepage: www.elsevier.com/locate/dyepig

Short communication

# A near-infrared and colorimetric fluorescent probe for palladium detection and bioimaging

Wei Su, Biao Gu, Xiaojun Hu, Xiaoli Duan, Youyu Zhang, Haitao Li*, Shouzhuo Yao

*Key Laboratory of Chemical Biology and Traditional Chinese Medicine Research (Ministry of Education), College of Chemistry and Chemical Engineering, Hunan Normal University, Changsha 410081, China*

ARTICLE INFO

*Article history:*
Received 21 September 2016
Received in revised form
31 October 2016
Accepted 31 October 2016
Available online 3 November 2016

*Keywords:*
Near-infrared
Fluorescent probe
Palladium
Bioanalytical applications

ABSTRACT

A near-infrared (NIR) and colorimetric fluorescent probe was developed for palladium species *via* a palladium catalyzed deallylation reaction. In this probe, 6-hydroxy-2,3-dihydro-xanthene-indolium (**CyH**) was acted as the signal unit and an allyl carbonate group was acted as the recognition unit. This non-fluorescent probe molecule can release the relevant fluorophore after interaction with palladium. The sensing mechanism was investigated by optical spectrum and NMR spectra. The probe can be used for "naked-eye" detection of palladium, and exhibited high selectivity to palladium over various other metal ions. Furthermore, the probe can be applied to imaging intracellular palladium ions in living HeLa cells, indicating its great potential for in *vivo* bioanalytical applications.



## 1. Introduction

Palladium (Pd) as a precious metal was widely used in various materials and pharmacy such as catalytic converters, fuel cells, jewelry, dental crowns and so on [1–3], which led to high level of residual palladium in the final product [4–6], thus resulting in fearful environmental and health problems because it can bind to biomolecules like proteins, DNA, thiol-containing amino acids and disturb cellular processes [7–9]. Therefore, development of efficiency methods for detective and imaging palladium species is important for environment safe and human health.

Up to now, there are many traditional methods reported for the detection of palladium species [10–13], such as inductively coupled plasma atomic emission spectrometry (ICP-AES), solid-phase microextraction high performance liquid chromatography (SPME-HPLC), X-ray, atomic absorption spectroscopy (AAS), *etc* [14–17]. However, they suffer from complicated sample preparation procedures, complicated instrumentation and the requirement for highly-trained individuals [18–20]. Compared with above technologies, fluorometry is more attractive due to excellent sensitivity, high selectivity, low detection limit and operational simplicity [21–24].

In the past few years, several fluorescent probes have been reported for the detection of palladium. For example, M. Kumar et al. design a fluorescent probe detection of palladium based on hydroxyphenyl-benzothiazole [25]. And Liu et al. prepared a "*turn-on*" fluorescent probe for palladium using rhodamine as the signal group [26]. However, these probes need the ultraviolet or visible light to excite, which severely limits in biological applications because the fluorescence imaging in the visible region would be easily disturbed by cell auto-fluorescence in living systems [27–32]. Therefore, it is consequential to develop the near infrared fluorescent probes for the detection of palladium [33]. Recently, Wang's group has design a near-infrared fluorescent probe for palladium, which exhibits high sensitivity and selectivity toward both Pd(0) and Pd(II). But this probe has a main drawback of poor water solubility, which is a disadvantage for bioimaging application [34]. Zhang' group reported a fluorescent probe for palladium. Although this probe emit in the red light region, it cannot be used for monitoring palladium in living cells due to the need high proportion of organic solvents [35]. Until now, the fluorescent probe based on near-infrared dyes for imaging intracellular palladium is very rare. In addition, colorimetric method has also draw much attention in terms of practical application due to its low-cost and convenient operations [36]. As a consequence, it is still urgently demanded to develop a novel NIR and colorimetric fluorescent probe for sensing palladium species in biological sample.

Based on above consideration, we choose heptamethine cyanine

* Corresponding author.
*E-mail address:* hatiao-li@hunnu.edu.cn (H. Li).

http://dx.doi.org/10.1016/j.dyepig.2016.10.052
0143-7208/

derivative (**CyH**) as the chromophore due to its NIR-emission, excellent water solubility, easily synthetic and predictable colour change in the solution after modification [37,38]. Herein, we designed and synthesized a new NIR and colorimetric fluorescent probe, 6-((allylcarbonyl)oxy)-2,3-dihydro-xanthenes-indolium (**CyPd**) detection of palladium. The probe is composed of **CyH** as the fluorophore and the allyl carbonate group as the recognition unit (in Scheme 1). In absence of any analyte, the free **CyPd** has almost no fluorescence due to the intermolecular charge transfer (**ICT**) possess from the fluorophore to the allyl carbonate group. Upon addition of palladium, the depropargylation reaction occurs and thus the protected hydroxyl group on the **CyPd** is liberated, which lead to the significant enhancement of fluorescence. Indeed, the synthesized probe showed many advantages as follow: high selective and sensitive to palladium; emission in the NIR light region ($\lambda_{em}$ = 721 nm); excellent water solubility; simple synthesis; "naked-eye" detection for palladium; the capability of monitoring palladium in living cells. All of these performances make it appropriate for potential application in biology.

## 2. Experimental sections

### 2.1. Reagents and apparatus

2,3,3-trimethyl-3H-indole, cyclohexanone, phosphoryl chloride, sodium acetate, resorcinol, potassium carbonate, triethylamine, allyl carbonochloridate, $Pd(PPh_3)_4$ (Pd(0)), $PdCl_2$ (Pd(II)) and $(NH_4)_2PdCl_6$ (Pd(IV)) were purchased from Energy Chemical. Acetonitrile (ACN), Chloroform, Dimethyl formamide (DMF), Dichloromethane (DCM), Dimethyl sulfoxide (DMSO), and Acetic anhydride were obtained from Sinopharm Chemical Reagent Company. All chemicals used in this work were of analytical grade and without further purification. Double distilled water was used in this work.

Electrospray mass spectrometry (ESI-MS) spectra were acquired on a ZQ2000 mass spectrometer (Manchester, UK). $^1H$ and $^{13}C$ nuclear magnetic resonance (NMR) spectra were recorded on a Bruker AVB-500 spectrometer using TMS as an internal standard. UV–vis spectra were recorded on a UV-2450 spectrophotometer (Shimadzu). Time dependent fluorescence spectra were recorded at 37 °C on a QM40 fluorescence spectrophotometer (PTI, Canada), and other fluorescence spectra were recorded at room temperature using an F-7000 fluorescence spectrophotometer (Hitachi Co., Japan) with the excitation and emission slit widths at 5 nm.

### 2.2. Synthesis of compounds

The synthetic route of **CyPd** is shown in Scheme 2. The resulting compounds were characterized by conventional ESI-MS, $^1H$ NMR, and $^{13}C$ NMR spectroscopy (see Fig. S1–S8).

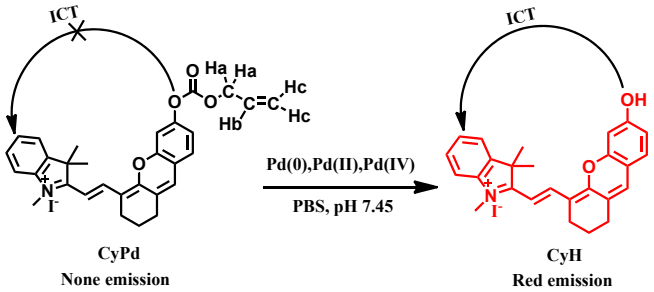


**Scheme 1.** Recognition mechanism of **CyPd** toward palladium.

#### 2.2.1. Synthesis of compound *1*

Compound 1 was synthesized on the basis of the procedures reported in the literature [39]. A mixture of dimethylformamide (40 mL) and methylene chloride (40 mL) was chilled in an ice bath for 30 min. Then phosphorus oxychloride (37 mL, 0.41 mol) and cyclohexanone (10.0 g, 0.10 mol) was added dropwise to the above mixture solution with stirring. The mixture solution was refluxed for 3 h, cooled, poured onto 300 g of ice, and stand to overnight. The yellow solid was collected with a yield of 7.8 g (44.5%).

#### 2.2.2. Synthesis and characterization of *Cy-7*

2,3,3-trimethyl-3H-indole (3.66 g, 11.66 mmol), compound 1 (0.96 g, 5.44 mmol) and sodium acetate (0.47 g, 5.44 mmol) were dissolved in 30 mL acetic anhydride under nitrogen atmosphere. The mixture solvent was stirred for 2 h at room temperature. Then the mixture solvents were removed under vacuum. The residual were washed with ether to obtain 3.2 g of pure green solid (91%). $^1H$ NMR (500 MHz, $CDCl_3$): $\delta$ 8.31 (d, $J$ = 14.1 Hz, 2H), 7.40–7.33 (m, 4H), 7.24–7.14 (m, 4H), 6.18–6.15 (s, 2H), 3.72 (s, 6H), 2.70 (t, $J$ = 6.1 Hz, 4H), 1.97–1.88 (m, 2H), 1.69 (s, 12H); $^{13}C$ NMR (126 MHz, $CDCl_3$): $\delta$ 172.90, 150.67, 144.38, 142.75, 140.89, 128.84, 127.65, 125.36, 122.15, 110.88, 101.60, 77.40, 77.15, 76.90, 49.25, 32.69, 29.66, 28.08, 26.73, 20.68.

#### 2.2.3. Synthesis and characterization of *CyH*

A stirred solution of resorcinol (220 mg, 2.0 mmol) and $K_2CO_3$ (276 mg, 2.0 mmol) in 15 mL ACN at room temperature under nitrogen atmosphere, stirred for 20 min, a solution of ACN (10 mL) contain compound 2 (610 mg, 1.0 mmol) was added to the above mixture solution *via* a syringe. The mixture solution was heated for 4 h at 50 °C. The solvent was evaporated under reduced pressure, the crude product was purified by silica gel column chromatography ($CH_2Cl_2/CH_3OH$ = 50:1), contain the desired **CyH** as a blue-green solid (373 mg, yield 73%). $^1H$ NMR (500 MHz, DMSO-$d_6$): $\delta$ 8.15 (d, $J$ = 13.9, 1H), 7.56 (s, 1H), 7.53 (d, $J$ = 7.3, 1H), 7.37 (t, $J$ = 9.3, 2H), 7.28 (d, $J$ = 7.9, 1H), 7.17 (t, $J$ = 7.4, 1H), 6.59 (d, $J$ = 8.9, 1H), 6.44 (s, 1H), 6.01 (d, $J$ = 13.8, 1H), 3.55 (s, 3H), 2.64 (d, $J$ = 17.9, 2H), 2.63 (t, $J$ = 5.6 Hz, 2H), 1.79 (s, 2H), 1.66 (s, 6H). $^{13}C$ NMR (126 MHz, DMSO-$d_6$): $\delta$ 169.76, 159.61, 143.83, 140.60, 138.46, 135.96, 130.38, 128.76, 123.96, 123.22, 122.60, 119.65, 115.88, 115.59, 110.42, 102.75, 98.32, 48.34, 40.50, 40.34–40.09, 40.00, 39.84, 39.67, 39.50, 31.25, 28.34, 28.01, 24.37, 21.10. MS (EI) $m/z$: 384.23 ($M^+$).

#### 2.2.4. Synthesis and characterization of *CyPd*

To a stirred solution of **CyH** (102.2 mg, 0.2 mmol, 1.0 equiv) in $CH_2Cl_2$ (10 mL) was added triethylamine ($Et_3N$, 56 μL, 0.4 mmol, 2.0 equiv) and allyl chlorocarbonate (42.42 μL, 0.4 mmol, 2.0 equiv) at 0 °C under nitrogen atmosphere. Stirred for 30 min, the mixture was heated to room temperature and stirred overnight. the reaction mixture was concentrated under reduced pressure to give crude solid, then purified by silica gel column chromatography ($CH_2Cl_2/CH_3OH$ = 50:1) to afford desired probe **CyPd** as a blue solid (51 mg, yield 43%). $^1H$ NMR (500 MHz, DMSO-$d_6$): $\delta$ 8.56 (d, $J$ = 15.3 Hz, 1H), 7.78 (d, $J$ = 7.4 Hz, 1H), 7.74 (d, $J$ = 7.9 Hz, 1H), 7.58 (t, $J$ = 10.1 Hz, 3H), 7.51 (t, $J$ = 7.3 Hz, 1H), 7.38 (s, 1H), 7.22 (dd, $J$ = 8.4, 2.2 Hz, 1H), 6.66 (d, $J$ = 15.3 Hz, 1H), 6.03 (ddd, $J$ = 22.8, 10.7, 5.7 Hz, 1H), 5.44 (dd, $J$ = 17.2, 1.5 Hz, 1H), 5.34 (dd, $J$ = 10.5, 1.2 Hz, 1H), 4.78 (d, $J$ = 5.6 Hz, 2H), 3.94 (s, 3H), 2.75–2.70 (m, 2H), 2.68 (t, $J$ = 5.9 Hz, 2H), 1.87–1.80 (m, 2H), 1.75 (s, 6H). $^{13}C$ NMR (126 MHz, DMSO-$d_6$): $\delta$ 179.40, 158.85, 152.93, 152.76, 152.65, 145.51, 142.85, 142.64, 132.07, 130.56, 130.33, 129.33, 128.76, 128.23, 123.13, 120.20, 119.65, 119.04, 114.61, 114.26, 109.97, 107.37, 69.60, 51.25, 33.62, 29.15, 27.42, 24.01, 20.27. MS (EI) $m/z$: 468.20 ($M^+$).

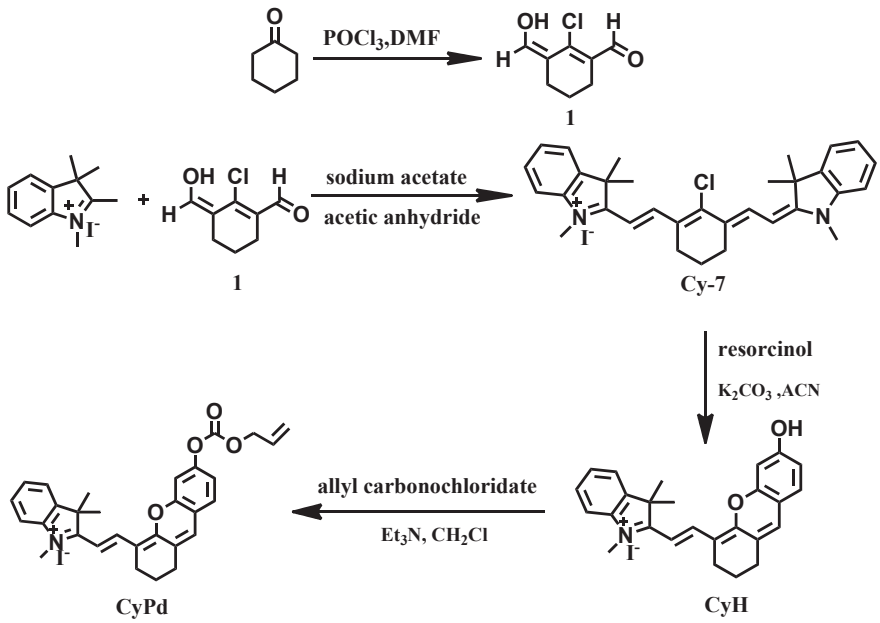


**Scheme 2.** Synthetic route of **CyPd.**

### 2.3. Analytical procedure

Stock solutions of **CyPd** (1.0 mM) and **CyH** (1.0 mM) were prepared in DMSO. Stock solutions of palladium species (1.0 mM) were prepared from Pd(0) in DMSO, and Pd(II), Pd(IV) prepared in water. Stock solutions of metal ions (20.0 mM) were prepared from $AgNO_3$, $FeCl_3 \cdot 6H_2O$, $FeCl_2 \cdot 4H_2O$, $BaCl_2 \cdot 2H_2O$, $AlCl_3$, $Pb(NO_3)_2$, $CaCl_2 \cdot 2H_2O$, $MgCl_2 \cdot 6H_2O$, $ZnCl_2$, $NiCl_2 \cdot 6H_2O$, $MnCl_2 \cdot 4H_2O$, $CdCl_2 \cdot 2.5H_2O$, NaCl, $CoCl_2 \cdot 6H_2O$, $CuCl_2 \cdot 2H_2O$, $HgCl_2$, LiCl and $SrCl_2 \cdot 6H_2O$ in water. Test solutions were prepared by dissolving 20 μL of **CyPd** stock solutions and a suitable amount of the analyte stock solution into a phosphate buffer solution (PBS, 10 mM, pH 7.4). The mixture (final volume is 2.0 mL containing 5.0% v/v DMSO) was incubated at 37 °C for 30 min, Then, the fluorescence emission spectra of the result solutions were recorded at an excitation wavelength of 670 nm (unless otherwise noted, all spectral were measured according to this method).

### 2.4. Cell cultures and fluorescence imaging

The HeLa cells were cultivated on a 96-well plate in the cultivate medium and allowed to adhere for 24 h at 37 °C. The cells were washed with phosphate buffered saline (PBS) and incubated with 5 μM **CyPd** for 30 min at 37 °C, then washed with PBS for three times, and imaged. After incubating with 5 μM Pd for another 1 h at 37 °C, the HeLa cells were washed three times with PBS and imaged again. Fluorescence imaging of intracellular Pd in HeLa cells was recorded on an inverted fluorescence microscope (Nikon, Eclipse Ti–S) with a 40 × objective lens. The excitation wavelength of the laser was 540 nm.

## 3. Results and discussion

### 3.1. Spectral characteristics

The optical properties of **CyPd** were measured in 10 mM PBS buffer ($H_2O$/DMSO = 19:1, v/v, pH = 7.4) with or without Pd(0). As shown in Fig. 1, **CyPd** showed weak absorption and weak fluorescence. However, the absorbance increased significantly after adding Pd(0) (0.5 and 1.0 μM) (Fig. 1A). Meanwhile, the fluorescence signal of **CyPd** displayed obvious changes after adding Pd(0) (0.5 and 1.0 μM) (Fig. 1B). And the colour change from blue to cyan after addition of Pd(0) (0.0, 0.05, 0.10 μM) (see Fig. 1A inset).

Then, we investigate the kinetic profiles of the reaction, in order to clarify the process of deallylation reaction. The responding of **CyPd** to palladium was prove when added palladium species with different valence states to the **CyPd**, as show in Fig. 2, The result revealed that **CyPd** responds to palladium species in the following rules: Pd(0) > Pd(II) > Pd(IV). Thus, Pd(0) was selected as the representative palladium species in the following experiments.

### 3.2. Mechanism study

New fluorescent probe **CyPd** contains a **CyH** as the signal unit and an allyl carbonate group as the sensing unit. In **CyPd**, **CyH** was weak absorption and fluorescence emission under the protection of the −OH group with an allyl carbonate group. However, the allyl carbonate group was left after incubated by Pd(0), the −OH group in the probe will be released, and results in strong absorption and fluorescent emission. The absorption and emission of **CyPd** in the absence and presence of Pd(0) was investigated. As shown in Fig. S9, the **CyPd** exhibited weak absorption and emission in the absence of Pd(0). The absorbance and the emission were increased notably after **CyPd** was treated with Pd(0), and the absorption and emission spectrum was the same as **CyH**. Thus, these results indicated that **CyPd** undergo the deallylation reaction followed by hydrolysis to generate **CyH**. The strong absorption and emission of **CyH** at longer wavelength possible resulted from intermolecular charge transfer (ICT). It is well known that the emission spectra of molecules possessing the intermolecular charge transfer (ICT) process show obvious red-shift with the increase of the polarity of solvent. In order to better understand the mechanism in our work, we examined the effect of polarity of solvents on the fluorophore **CyH**. As shown in Fig. S10, the maximal emission of **CyH** displayed red-shift from 685 nm to 737 nm (from DCM to MeOH), which suggest the character of the ICT process in the **CyH** structure. However, after the introduction allyl carbonate group to the beckon of **CyH**, the ICT efficiency in the resulting probe molecule was

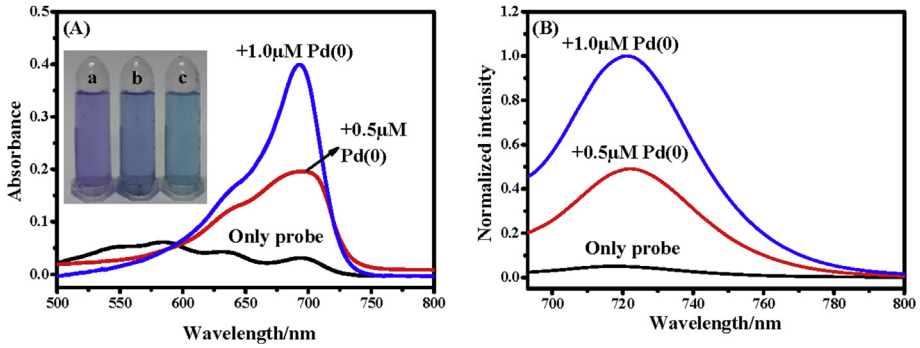


**Fig. 1.** UV– vis (A) and Fluorescence emission (B) spectra of **CyPd** (10 μM), reacting with Pd(0) (0, 0.5, 1.0 μM) in 10 mM PBS buffer ($H_2O$/DMSO = 19:1, v/v, pH = 7.4, 37 °C, $\lambda_{ex}$ = 670 nm). Inset image: (a) visible-light image of 10 μM probe; (b) visible-light image of 10 μM probe and 0.5 μM Pd(0); (c) visible-light image of 10 μM probe and 1.0 μM Pd(0).

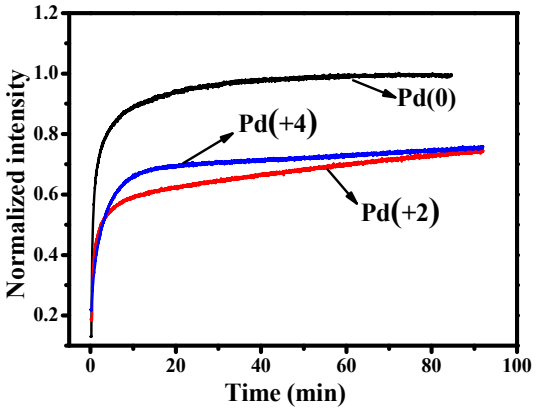


**Fig. 2.** Time-dependent fluorescence changes of **CyPd** (10 μM) in the presence of three palladium species (5.0 μM) in 10 mM PBS buffer ($H_2O$/DMSO = 19:1, v/v, pH = 7.4, 37 °C, $\lambda_{ex}$ = 670 nm).

weaken, leading to the fluorescence quenching. Furthermore, compared with a similar probe molecule in the reported literature [37], it was found that the absorption change of referent probe is similar as ours. Thus, the detection in our work is more likely to be determined by the ICT process.

In order to further verify the above reaction mechanism, the product of **CyPd** was isolated by a silica gel column after interaction with Pd(0), and then was characterized by $^1$HNMR spectra. As shown in Fig. 3, **CyPd** shows the characteristic alkenyl proton $H_b$ and $H_c$ from 4.5 to 5.5 ppm and methylene proton $H_a$ at 6.0 ppm, respectively.

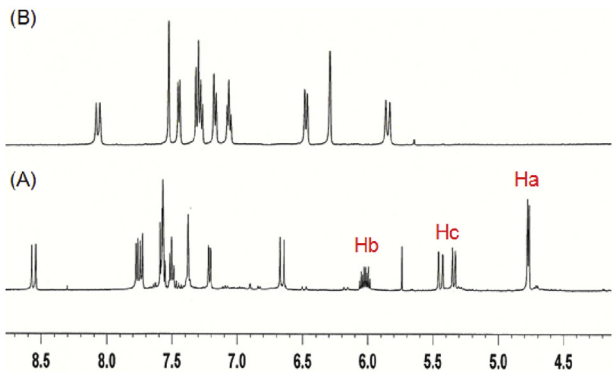


**Fig. 3.** $^1$H NMR (500 MHz) spectra of **CyPd** (A) and the isolated product of **CyPd** + Pd(0) (B) in DMSO.

However, the peak of the vinyl group in the product disappeared, which indicated that **CyPd** undergoes the deallylation reaction followed by hydrolysis to generate the **CyH** (Fig. S11).

### 3.3. Effects of pH and incubation time

In order to obtain a excellent-sensitive response for Pd(0), the effects of the experimental parameters, like pH and incubation time were investigated. Fig. S12A illustrates the effect of pH on fluorescence properties of **CyPd** and it response to Pd(0). The pH value had no obvious effect on the fluorescence intensity of **CyPd** itself, however, it was notable that the fluorescence intensity increased in the presence of Pd(0) in pH range from 5.0 to 7.45, and then reached a constant value at alkaline condition. These results indicated that the alkaline conditions in favour of the deallylation reaction. Therefore, physiological pH (pH = 7.4) could be act as an appropriate working pH in the following experiments. Fig. S12B shows the time dependent fluorescence response of **CyPd** in the absence and presence of Pd(0), suggesting that the reaction between **CyPd** and Pd(0) was completed within 30 min. Hence, the incubation time was controlled at 30 min.

### 3.4. Pd detection performance

Under the optimal conditions, we studied the analysis capabilities of **CyPd** by fluorescence response towards various concentrations of Pd(0). As shown in Fig. 4A, the fluorescence intensity at 721 nm increased with the increasing concentrations of Pd(0). The normalized emission intensity ($\lambda_{ex}$ = 721 nm) was linearly proportional to the concentrations of Pd(0) in the range of 0–1.0 μM (Fig. 4B). A linear regression equation for Pd(0), $F = 0.0168 + 0.9702x$ ($R^2 = 0.9966$), was obtained, where $F$ refers to the normalized intensities and $x$ refers to the concentration of Pd(0). The limit of detection (LOD) ($S/N$ = 3, the concentration necessary to yield a net signal equal to three times the standard deviation of the background) was calculated to be $2.24 \times 10^{-8}$ M. These results revealed that **CyPd** could monitor Pd(0) levels both qualitatively and quantitatively. In addition, the increase of the absorbance intensity at 695 nm corresponded to the addition of Pd(0) to the **CyPd** (Fig. S13).

It is most important that a highly selective response to the target species over other potentially competing species for a new fluorescent probe with potential application in complex biological and environmental samples. Therefore, the selectivity of **CyPd** to Pd was investigated. As shown in Fig. 5, there was no notably fluorescence change in the presence of the common cations, such as $Ag^+$, $Fe^{3+}$, $Fe^{2+}$, $Ba^{2+}$, $Al^{3+}$, $Pb^{2+}$, $Ca^{2+}$, $Mg^{2+}$, $Zn^{2+}$, $Ni^{2+}$, $Mn^{2+}$, $Cd^{2+}$, $Na^+$, $Co^{2+}$, $Cu^{2+}$, $Hg^{2+}$, $Li^+$, and $Sr^{2+}$ (10 μM for Pd(0), 100 μM for other

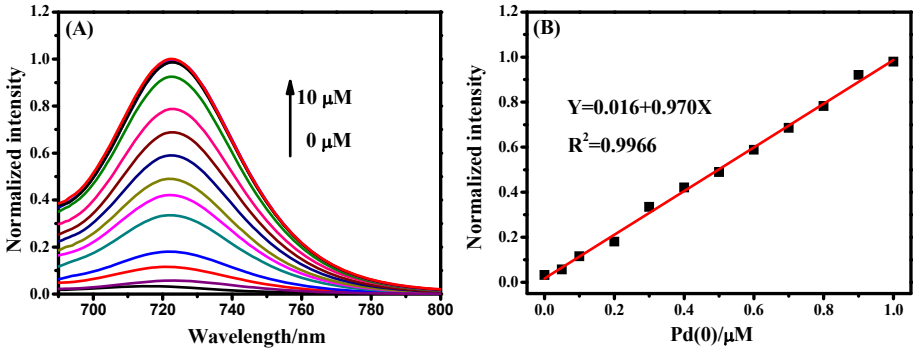


**Fig. 4.** Fluorescence spectrum evolution (A) of **CyPd** (10 μM) in the presence of different concentrations of Pd(0) (0–10 μM). Ratiometric calibration curve (B) of $I_{670\ nm}$ as a function of concentration of Pd(0), spectra were recorded in 10 mM PBS buffer ($H_2O$/DMSO = 19:1, v/v, pH = 7.4, 37 °C, $\lambda_{ex}$ = 670 nm).

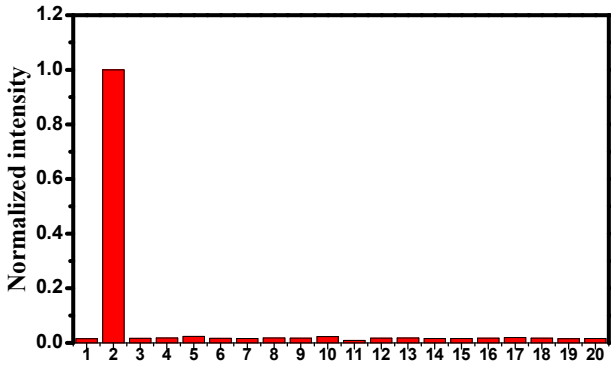


**Fig. 5.** Fluorescence responses of **CyPd** (10 μM) in the presence of different various cations (10 μM for Pd(0), 100 μM for other metal ions) (from left to right: blank, Pd(0), $Ag^+$, $Fe^{2+}$, $Fe^{3+}$, $Ba^{2+}$, $Al^{3+}$, $Pb^{2+}$, $Ca^{2+}$, $Mg^{2+}$, $Zn^{2+}$, $Ni^{2+}$, $Mn^{2+}$, $Cd^{2+}$, $Na^+$, $Co^{2+}$, $Cu^{2+}$, $Hg^{2+}$, $Li^+$, and $Sr^{2+}$, respectively) in 10 mM PBS buffer ($H_2O$/DMSO = 19:1, v/v, pH = 7.4, 37 °C, $\lambda_{ex}$ = 670 nm).

metal ions). However, a much larger fluorescence enhancement were observed for **CyPd** upon addition of Pd(0). These results clearly demonstrated that **CyPd** was a highly selective fluorescent probe for Pd, and also verified that the hydrolysis of allyl carbonate was specific toward Pd. In addition, the significant increase of the emission intensity at 721 nm, along with the apparent colour change only corresponding to the addition of Pd to the **CyPd** (Fig. S14), the result indicated that **CyPd** can be detection of Pd by naked-eye.

### 3.5. Detection of Pd in living cells

To further investigate the membrane permeability of **CyPd**, and its ability to detect palladium in living cells, the cell imaging experiment was carried out. Because $PdCl_2$ is the most toxic species among the palladium species, so we selected $PdCl_2$ as the representative palladium species in the cell fluorescent imaging experiment. As shown in Fig. 6, the cell fluorescence images displayed enhanced red fluorescence for the incubated HeLa cells with **CyPd** + $PdCl_2$ at 540 nm excitation, which the relative emission intensity was more intense compared to HeLa cells with **CyPd** (Fig. 6B and D). These results indicated that **CyPd** was cell-permeable and capable of imaging $PdCl_2$ in living cells. The bright-field images (Fig. 6A and C) confirmed that the cells were living throughout the imaging experiments. Moreover, the cytotoxicity of $PdCl_2$ in HeLa cells were investigated, the results from MTT assays showed that the cells remained higher viability upon treatment with 2.0–10.0 μM $PdCl_2$ for as long as 24 h (Fig. S15),

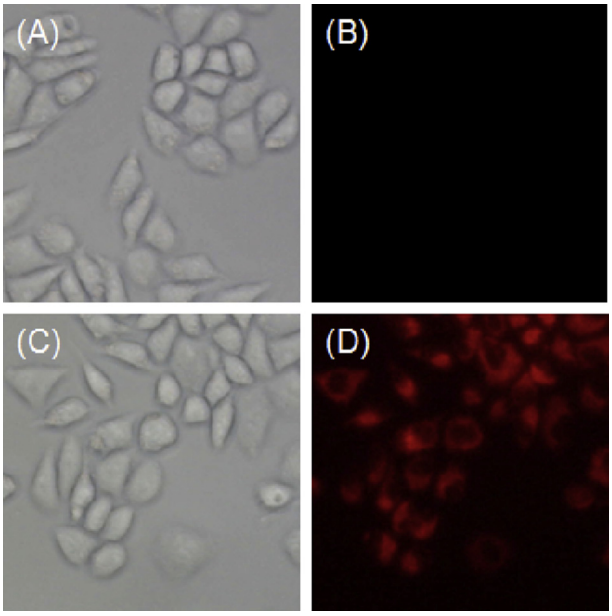


**Fig. 6.** Brightfield and fluorescence images of HeLa cells with **CyPd**: bright-field (A) and fluorescence image (B) of the cells only incubated with **CyPd** (5 μM) for 30 min; bright-field (C) and fluorescence image (D) of the cells incubated with **CyPd** (5 μM) for 30 min, and then addition of $PdCl_2$ (5 μM) for another 1 h.

indicating that $PdCl_2$ was low cytotoxicity to the living cells within a short time.

## 4. Conclusion

In summary, a new near-infrared and colorimetric fluorescent probe **CyPd** for palladium detection was successfully designed and synthesized based on heptamethine cyanine dye derivative. The probe exhibited high sensitivity and selectivity toward palladium with excellent water solubility. In addition, the probe can be used for "naked-eye" detection of palladium. Furthermore, **CyPd** has been successfully applied to imaging of palladium in HeLa cells. This research has demonstrated the potential of the probe for environmental and biological applications.

## Acknowledgments

This work was supported by the National Natural Science Foundation of China (21375037, 21475043 and 21275051), Doctoral Fund of Ministry of Education of China (NO: 20134306110006).

## Appendix A. Supplementary data

Supplementary data related to this article can be found at http://dx.doi.org/10.1016/j.dyepig.2016.10.052.

## References


[1] Chen H, Lin W, Yuan L. Construction of a near-infrared fluorescence turn-on and ratiometric probe for imaging palladium in living cells. Org Biomol Chem 2013;11:1938–41.
[2] Garner AL, Koide K. Studies of a fluorogenic probe for palladium and platinum leading to a palladium-specific detection method. Chem Commun 2009:86–8.
[3] Garner AL, Koide K. Fluorescent method for platinum detection in buffers and serums for cancer medicine and occupational hazards. Chem Commun 2009:83–5.
[4] Cho D-G, Sessler JL. Modern reaction-based indicator systems. Chem Soc Rev 2009;38:1647–62.
[5] Carey JS, Laffan D, Thomson C, Williams MT. Analysis of the reactions used for the preparation of drug candidate molecules. Org Biomol Chem 2006;4:2337–47.
[6] Shao L, Zhang B, Zhang W, Hong SY, Schlögl R, Su DS. The role of palladium dynamics in the surface catalysis of coupling reactions. Angew Chem Int Ed 2013;52:2114–7.
[7] Gunn SWA. World health organization. World J Surg 2004;28. 845–845.
[8] Kielhorn J, Melber C, Keller D, Mangelsdorf I. Palladium-a review of exposure and effects to human health. Int J Hyg Environ Health 2002;205:417–32.
[9] Yusop RM, Unciti-Broceta A, Johansson EM, Sánchez-Martín RM, Bradley M. Palladium-mediated intracellular chemistry. Nat Chem 2011;3:A48–50.
[10] Dodani SC, He Q, Chang CJ. A turn-on fluorescent sensor for detecting nickel in living cells. J Am Chem Soc 2009;131:18020–1.
[11] Domaille DW, Zeng L, Chang CJ. Visualizing ascorbate-triggered release of labile copper within living cells using a ratiometric fluorescent sensor. J Am Chem Soc 2010;132:1194–5.
[12] Jung HS, Kwon PS, Lee JW, Kim JI, Hong CS, Kim JW, et al. Coumarin-derived $Cu^{2+}$-selective fluorescence sensor: synthesis, mechanisms, and applications in living cells. J Am Chem Soc 2009;131:2008–12.
[13] Nolan EM, Lippard SJ. Tools and tactics for the optical detection of mercuric ion. Chem Rev 2008;108:3443–80.
[14] Kaur V, Aulakh JS, Malik AK. A new approach for simultaneous determination of Co(II), Ni(II), Cu(II) and Pd(II) using 2-thiophenaldehyde-3-thiosemicarbazone as reagent by solid phase microextraction–high performance liquid chromatography. Anal Chim Acta 2007;603:44–50.
[15] Locatelli C, Melucci D, Torsi G. Determination of platinum-group metals and lead in vegetable environmental bio-monitors by voltammetric and spectroscopic techniques: critical comparison. Anal Bioanal Chem 2005;382:1567–73.
[16] Petrova PP, Velichkov SV, Havezov IP, Daskalova NN. Inductively coupled plasma atomic emission spectrometry-line selection and accuracy in the determination of platinum, palladium, rhodium, barium and lead in automotive catalytic converters. Bulg Chem Commun 2009;41:65–71.
[17] Van Meel K, Smekens A, Behets M, Kazandjian P, Van Grieken R. Determination of platinum, palladium, and rhodium in automotive catalysts using high-energy secondary target X-ray fluorescence spectrometry. Anal Chem 2007;79:6383–9.
[18] Benkhedda K, Dimitrova B, Infante HG, Ivanova E, Adams FC. Simultaneous on-line preconcentration and determination of Pt, Rh and Pd in urine, serum and road dust by flow injection combined with inductively coupled plasma time-of-flight mass spectrometry. J Anal A. T Spectrom 2003;18:1019–25.
[19] Dimitrova B, Benkhedda K, Ivanova E, Adams F. Flow injection on-line preconcentration of palladium by ion-pair adsorption in a knotted reactor coupled with electrothermal atomic absorption spectrometry. J Anal A. T Spectrom 2004;19:1394–6.
[20] Feldmann I, Jakubowski N, Stuewer D. Application of a hexapole collision and reaction cell in ICP-MS part I: instrumental aspects and operational optimization. Fresenius J Anal Chem 1999;365:415–21.
[21] Du J, Hu M, Fan J, Peng X. Fluorescent chemodosimeters using "mild" chemical events for the detection of small anions and cations in biological and environmental media. Chem Soc Rev 2012;41:4511–35.
[22] Meng Z, Qin G, Zhang B, Bai J. DNA damaging effects of sulfur dioxide derivatives in cells from various organs of mice. Mutagenesis 2004;19:465–8.
[23] Su D, Oh J, Lee S-C, Lim JM, Sahu S, Yu X, et al. Dark to light! a new strategy for large stokes shift dyes: coupling of a dark donor with tunable high quantum yield acceptors. Chem Sci 2014;5:4812–8.
[24] Yang Y, Zhao Q, Feng W, Li F. Luminescent chemodosimeters for bioimaging. Chem Rev 2012;113:192–270.
[25] Kumar M, Kumar N, Bhalla V. Highly selective fluorescent probe for detection and visualization of palladium ions in mixed aqueous media. RSC Adv 2013;3:1097–102.
[26] Balamurugan R, Chien C-C, Wu K-M, Chiu Y-H, Liu J-H. A depropargylation-triggered fluorescence "turn-on" probe for the detection of $Pd^{2+}$ based on a bispropargylamine-rhodamine conjugate. Analyst 2013;138:1564–9.
[27] Du X, Wang ZY. Donor-acceptor type silole compounds with aggregation-induced deep-red emission enhancement: synthesis and application for significant intensification of near-infrared photoluminescence. Chem Commun 2011;47:4276–8.
[28] Guo Z, Park S, Yoon J, Shin I. Cheminform abstract: recent progress in the development of near-infrared fluorescent probes for bioimaging applications. Chem Soc Rev 2014;43:16–29.
[29] Kartonlifshin N, Segal E, Omer L, Portnoy M, Satchifainaro R, Shabat D. A unique paradigm for a turn-on near-infrared cyanine-based probe: noninvasive intravital optical imaging of hydrogen peroxide. J Am Chem Soc 2011;133:10960–5.
[30] Li L, Li P, Fang J, Li Q, Xiao H, Zhou H, et al. Simultaneous quantitation of Na(+) and K(+) in single normal and cancer cells using a new near-infrared fluorescent probe. Anal Chem 2015;87:6057–63.
[31] Zhu D, Li G, Xue L, Jiang H. Development of ratiometric near-infrared fluorescent probes using analyte-specific cleavage of carbamate. Org Biomol Chem 2013;11:4577–80.
[32] Zhu W, Huang X, Guo Z, Wu X, Yu H, Tian H. A novel NIR fluorescent turn-on sensor for the detection of pyrophosphate anion in complete water system. Chem Commun 2012;48:1784–6.
[33] Wang J, Song F, Wang J, Peng X. A near-infrared and ratiometric fluorescent chemosensor for palladium. Analyst 2013;138:3667–72.
[34] Wang P, Xia J, Gu Y. A novel NIR fluorescent probe for palladium detection based on Pd(0) mediated reaction. Tetrahedron Lett 2015;56:6491–4.
[35] Xiang K, Liu Y, Li C, Tian B, Zhang J. A colorimetric and ratiometric fluorescent probe for detection of palladium in the red light region. RSC Adv 2015;5:52516–21.
[36] Jiang J, Jiang H, Liu W, Tang X, Zhou X, Liu W, et al. A colorimetric and ratiometric fluorescent probe for palladium. Org Lett 2011;13:4922–5.
[37] Zhang J, Ning L, Liu J, Wang J, Yu B, Liu X, et al. Naked-eye and near-infrared fluorescence probe for hydrazine and its applications in in vitro and in vivo bioimaging. Anal Chem 2015;87:9101–7.
[38] Zhang J, Wang J, Liu J, Ning L, Zhu X, Yu B, et al. Near-infrared and naked-eye fluorescence probe for direct and highly selective detection of cysteine and its application in living cells. Anal Chem 2015;87:4856–63.
[39] Wang L, Jin J, Chen X, Fan H-H, Li BKF, Cheah K-W, et al. A cyanine based fluorophore emitting both single photon near-infrared fluorescence and two-photon deep red fluorescence in aqueous solution. Org Biomol Chem 2012;10:5366–70.